IOSR Journal of Mechanical and Civil Engineering (IOSR-JMCE)
e-ISSN: 2278-1684,p-ISSN: 2320-334X, Volume 15, Issue 1 Ver. I (Jan. - Feb. 2018), PP 48-63
www.iosrjournals.org

Modelling Confined Hydrocarbon Gas Explosions Part I: Algorithm Development

Alon Davidy[1]
[1](Computational Engineering/IMI)
Corresponding Author: Alon Davidy

Abstract: *Unexpected releases of combustible vapors/gases can lead to explosions, which threaten the integrity of equipment and structures. Multiple explosions can destroy plants, jeopardize lives, and inflict large economic losses; outdated parts of the pipe system can leak flammable gas in air and pose the danger of explosion. Therefore, it is important to be able to predict explosion properties and to design pipes and storage tanks that can withstand such catastrophic events. Such efforts enable plant engineers to evaluate risks associated with their designs subject to various possible explosions. Pressure rises almost instantaneously because of the overpressure from an explosion causing structural damage or deformation of pipes and storage tanks. Explosive pressure and structural damage can be estimated with analytical and numerical tools. By using these computational tools, safe distances between equipment and structures can be assigned. In this work an algorithm has been developed in order to estimate the structural damage. The proposed algorithm is composed from the following steps: Calculation of the gaseous concentration field and mass by using FDS software, Calculation of the shock wave pressure loads on the walls & Estimation of structural integrity of the structure*.
Keywords - *Hydrocarbons, Gaseous concentration, Explosion, Detonation, Gaseq code, FDS code,*

Date of Submission: 02-01-2018 Date of acceptance: 18-01-2018

I. Introduction

Unexpected releases of combustible vapors/gases can lead to explosions, which threaten the integrity of equipment and structures [1]. Multiple explosions can destroy plants, jeopardize lives, and inflict large economic losses; outdated parts of the pipe system can leak flammable gas in air and pose the danger of explosion as illustrated in Figure 1 [1-3]. Therefore, it is important to be able to predict explosion properties and to design pipes and storage tanks that can withstand such catastrophic events. Such efforts enable plant engineers to evaluate risks associated with their designs subject to various possible explosions. Pressure rises almost instantaneously because of the overpressure from an explosion causing structural damage or deformation of pipes and storage tanks. Explosive pressure and structural damage can be estimated with analytical and numerical tools. By using these computational tools, safe distances between equipment and structures can be assigned.

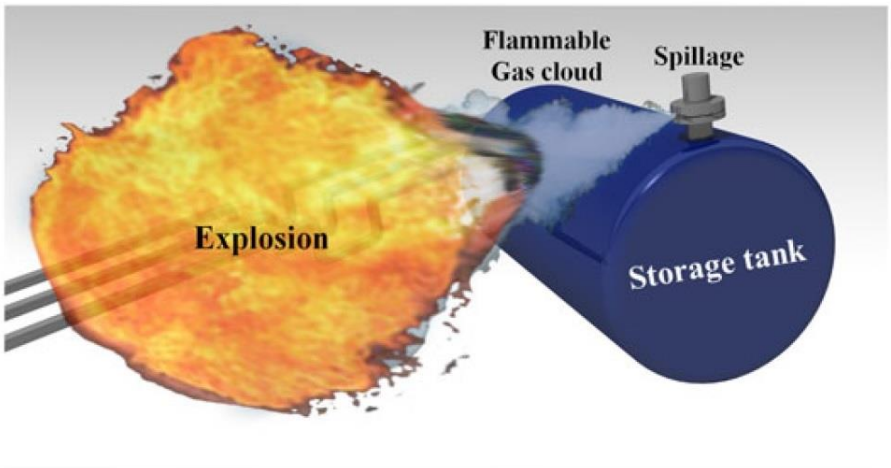

Fig. 1: Schematic of an explosion and its effects [1].

The earliest observations of detonation waves in gases were made by Berthelot & Vielle [4] and Mallard & La Chatelier [5]. While studying the propagation of flames in tubes they found that under certain conditions combustible gas mixtures propagate flames in tubes with speeds far greater than had been measured previously. The propagation reaches enormous velocities, from 1,000 to 3,500 m/sec, depending on the gas mixture, or many times the velocity of sound at ordinary temperatures and pressures [6]. Detonation waves are shock waves which are sustained by the chemical reaction that is initiated by the shock compression. They develop from flames in tubes by coalescence of flame-generated pressure pulses into shock waves, and they propagate spherically in suitably string mixtures when initiated by a small charge of high explosive. Their rate of propagation is limited by the rate at which a shock can travel, and hence it has been possible to develop the theory of propagation on the basis of hydrodynamics alone such extent that detonation velocities may be computed from the physical properties of the explosive medium. There are, however, other aspects of detonation phenomena which are only partially related to hydrodynamic processes and thus are out-side the scope of classical theory. These comprise transition from flame to detonation, limits of detonation, pulsation and spin of detonation waves. In addition, various problems arise from observations on the ignition of explosives by weak shocks, and from other incidental observations [6].

1.1 Characteristics of Explosion Properties of the Gas

The major explosion parameters of gases are:

1) Maximum pressure of explosion, p_{max}

2) Maximum rate of explosion pressure rise, $(dp/dt)_{max}$ (see figure 2) or K factor: $K = (dp/dt)_{max} V^{1/3}$

3) Explosion limits

4) Detonation limits

5) Temperature of self-ignition

6) Minimum energy of ignition

Fig. 2 shows the record of the explosion pressure in a closed container. The maximum pressure of explosion p_{max} is the highest pressure recorded during explosion in the closed container.

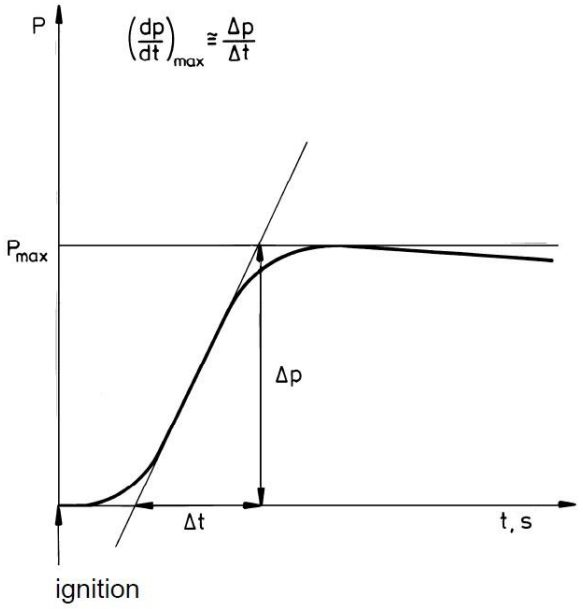

Fig. 2: Record of the explosion in a closed container.

1.2 Combustion properties of Gas – Air mixtures

The burning of a gas in air is a chemical reaction in which the fuel is oxidized releasing heat and often light. The chemical products of the complete combustion of hydrocarbon fuel are carbon dioxide and water vapor. Combustion of methane in air can be described by the reaction:

$$CH_4 + 2(O_2 + 3.762N_2) \rightarrow CO_2 + 2H_2O + 2(3.762N_2) + \text{heat} \qquad (1)$$

The temperature of premixed flame can be calculated from the (lower) heat of combustion of gas and the specific heats of combustion products. The flame temperature is highest for a stoichiometric mixture. This temperature is called the adiabatic flame temperature since it is calculated assuming the combustion to be an

adiabatic process (no heat losses to the environment). Table 1 presents the adiabatic flame temperatures $T_f[K]$ of some hydrocarbon gases and hydrogen in air [7].
The adiabatic flame temperature can be used to calculate the volume of stoichiometric mixture after the combustion has occurred. It follows from ideal gas law $pV = NRT$ that:

$$\frac{V_f}{V_i} = \frac{N_f T_f}{N_i T_i} \tag{2}$$

Where:
V_i is the initial volume in [m³]
V_f is the initial volume in [m³]
N_i is the number of moles in the unburned mixture in [mole]
N_f is the number of moles in the combustion products in [mole]
T_i is the initial temperature in [K]
For methane, the number of moles is conserved i.e. $N_f = N_i = 10.52$.
The ratio $E = V_f / V_i$ is called the expansion ratio of the gas. Values of the expansion factor E are given for hydrocarbon gases and hydrogen in table 1. For most hydrocarbon fuels, to a first approximation the mole number ratio N_f / N_i can be taken as 1. The expansion factor can be equated to the ratio of the temperatures T_f / T_i.

Table 1: Combustion properties of some hydrocarbon and hydrogen in air [7]

fuel	flamm. range %	stoich. mixt. %	T_f K	E	H_{st} MJ/m³
hydrogen	4 - 75	30	2318	8.0	3.06
methane	5 - 15	9.5	2148	7.4	3.23
ethane	3 - 12.5	5.6	2168	7.5	3.39
propane	2.2 - 9.5	4.0	2198	7.6	3.46
butane	1.9 - 8.5	3.1	2168	7.5	3.48
pentane	1.5 - 7.8	2.6	2232	7.7	3.59
hexane	1.2 - 7.5	2.2	2221	7.7	3.62
heptane	1.2 - 6.7	1.9	2196	7.6	3.62
acetylene	2.5 - 80	7.7	2598	9.0	3.93
ethylene	3.1 - 32	6.5	2248	7.8	3.64
propylene	2.4 - 10.3	4.4	2208	7.7	3.59
butylene	1.7 - 9.5	3.4	2203	7.6	3.64
benzene	1.4 - 7.1	2.7	2287	7.9	3.62
cyclohexane	1.3 - 8.0	2.3	2232	7.8	3.85

A basic quantity of premixed gas flames is the **burning velocity** - S_0. This is the velocity at which the flame front (thin reaction zone) travels in a laminar flow with respect to the unburned mixture immediately ahead of it. The flame front is stationary also in a burner for a premixed gas (see Fig. 3).

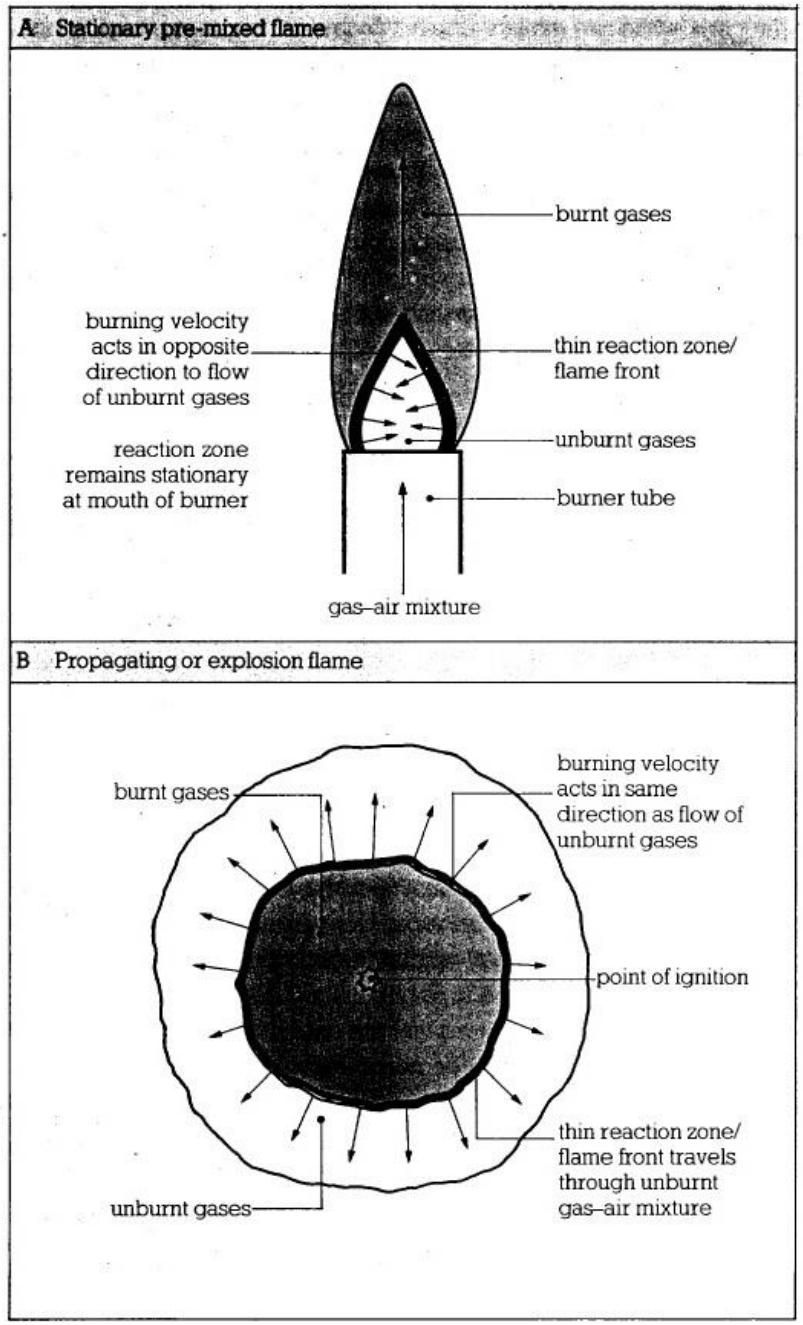

Fig. 3: Stationary and propagating flames [7]

The value of burning velocity is determined by the molecular transport processes, such as heat and mass transfer within the flame front. The burning velocity is a function of gas concentration, reaching a maximum just on the fuel rich side of the stoichiometric concentration (Figure 4). This maximum value and the corresponding concentration are given in table 2 for the gases in table 1. It is seen that the maximum laminar burning velocity of most hydrocarbon fuels is close to 0.5 m/s. Hydrogen has exceptionally large laminar burning velocity 3.5 m/s [7].

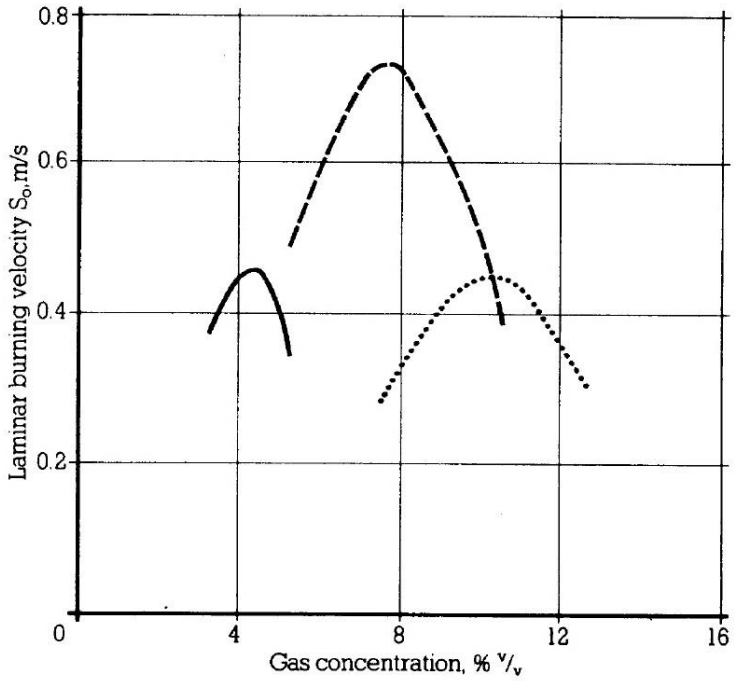

Fig. 4: Effect of gas concentration on burning velocity. Solid line = propane, dashed line = ethylene, dotted line = methane [7].

Table 2: Combustion properties of some hydrocarbon and hydrogen in air [7]

fuel	max S_o at %	max S_o m/s	max S_f m/s	AIT K	min. ign. energy mJ
hydrogen	54	3.5	28	847	0.02
methane	10	0.45	3.5	813	0.29
ethane	6.3	0.53	4.0	788	0.24
propane	4.5	0.52	4.0	723	0.25
butane	3.5	0.50	3.7	678	0.25
pentane	2.9	0.52	4.0	533	0.25
hexane	2.5	0.52	4.0	498	0.25
heptane	2.3	0.52	4.0	488	0.25
acetylene	9.3	1.58	14.2	578	0.02
ethylene	7.4	0.83	6.5	763	0.12
propylene	5.0	0.66	5.1	733	0.28
butylene	3.9	0.57	4.3	658	0.28
benzene	3.3	0.62	4.9	833	0.22
cyclohexane	2.7	0.52	4.1	518	0.24

Assuming that the gas cloud is initially at rest, the flow is laminar, the flame surface is smooth and that the burned gases are at all times trapped behind the expanding the flame front, the relationship between the flame speed and burning velocity can be expressed as:

$$S_f = ES_0 \tag{3}$$

Maximum values of the laminar flame speed, S_f have been calculated using Eq. (3) and are given in table 2. The adiabatic flame temperature, T_f and hence the expansion factor E depend on the concentration, having maximum at the stoichiometric mixture. It is concluded from Eq. (3) that the laminar flame speed S_f has the maximum close to the concentration at which the maximum burning velocity is measured. In reality, when a flame front propagates in any geometry it can develop a cellular structure showing peaks and troughs, often

collectively called wrinkles. These deviations from smooth surface can occur already when the flame radius is a few tens of centimeters. The volume production of burned gases, which expand to drive the flame front forward, is proportional to the actual surface area of the flame. This effect can be considered by adding an area correction term to Eq. (3) [7].

$$S_f = E\frac{A_f}{A_n}S_0 \tag{4}$$

Where

A_f is the actual flame area [m²]

A_n is the area of idealized (flame) flame [m²]

Unfortunately there is no simple method to predict the actual flame area, A_f. It is to be stressed that the burning velocity is fundamental property of any gas-air mixture, but the flame speed is not such. The flame speed, however, is a useful concept and the laminar flame speed is a lower limit to the real (turbulent) flame speed.

1.3 The generation of gas in gas explosions

When a gas cloud consisting of stoichiometric mixture burns outdoors the volume increases during the combustion (flash fire) by the expansion factor E. For most gases in table 1, this factor is close to 8. When a similar mixture fills a pressure fills a pressure vessel the absolute pressure in the vessel increases during the combustion (confined explosion) by the factor that is somewhat larger than E. Neglecting heat losses to the walls, the calculated pressure ratio p_f/p_i is about 9 (see Fig. 5). In an adiabatic processes, the pressure ratio would be $p_f/p_i = E$. The difference is caused by the compressive heating of unburned mixture and combustion products [7].

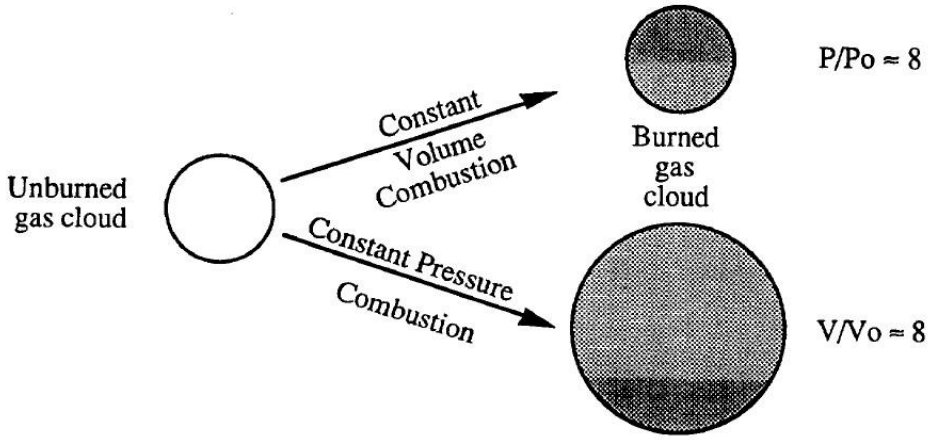

Fig. 5: constant volume and combustion pressure [7]

Figure 6 shows the overpressures in cubical vessel of 1 m³ calculated for stoichiometric mixtures of three gases. Heat losses to the walls are included. The rise time of the pressure depends on the burning velocity, S_0 and hence on the flame speed. Ethylene has the highest and methane the low burning velocity (table 2). Thus ethylene has the shortest and methane the longest rise time. Closed vessels have been used to measure explosion characteristics of flammable gas-air mixtures. Models for the time dependence of explosion overpressure in closed spherical vessels result in expressions for the rate rise in the form [7]

$$\frac{dp}{dt} = K_1\frac{S_0}{r_f} \tag{5}$$

Where:

K_1 is a constant [bar]

r_f is the radius of flame [m]

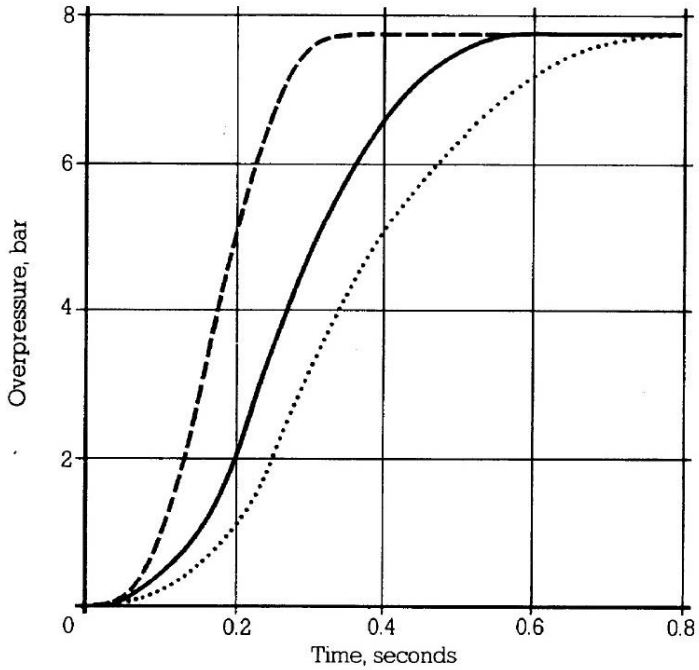

Fig. 6: Pressure-time curves for confined explosions in a cubical vessel of volume 1 m³. Dashed line = ethylene, solid line = propane, dotted line = methane [7].

Assuming that the maximum rate of pressure rise occurs at maximum flame area, r_f, can be replaced by the radius of the sphere, or equivalently cube root of its volume V [m³]

$$\left(\frac{dp}{dt}\right)_{max} = \frac{K_g}{V^{1/3}} \tag{6}$$

Eq. (4) is usually written in the form (called the **cube root law** or cubic law)

$$\left(\frac{dp}{dt}\right)_{max} V^{1/3} = K_g \tag{7}$$

The cube root law with experimental values of the constant $K_g[\text{bar}\cdot\text{m/s}]$ has been used to predict explosion overpressure in vented explosions [7].

A serious flaw in the use of the cube root law with an experimental value of K_g is that it does not include turbulence effects. An experiment performed in a small test vessel gives little information of the turbulence that can develop in large rooms due to instabilities and obstacles. Thus the constant K_g can't be considered a basic quantity of a given gas. On the other hand, the burning velocity S_0 is such a quantity and it has been shown to represent well the effect of gas reactivity on the pressure in vented explosions (British Gas 1990).

1.3 The Effect of Obstacles

Two effects can be identified by the presence of obstacles:

1) The flame front is distorted as it flows around the obstacles leading to an increase in the flame area (flame folding – see figure 7)
2) Turbulence is generated in the unburned mixture as it flows over and around the obstacles (see figure 8).

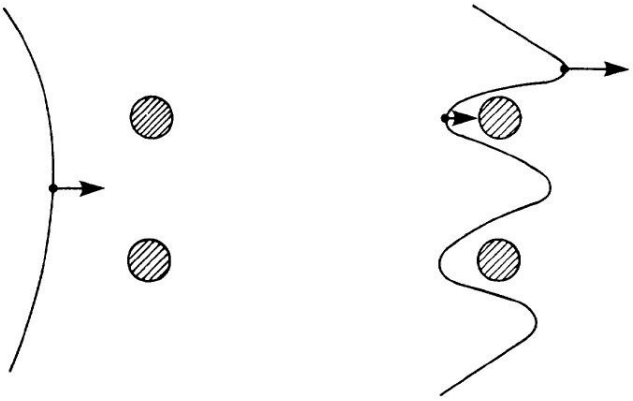

Fig. 7: Flame folding caused by obstacles [7].

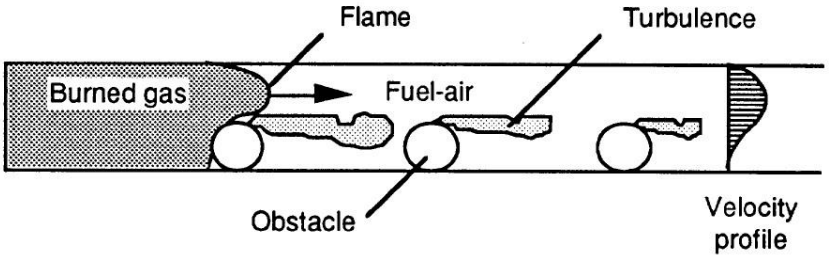

Fig. 8: Turbulence generation in the wake of obstacles [7]

The effect of repeated obstacles on flame speed is caused by the positive feedback loop shown in figure 9. Combustion of the unburned mixture is followed by the expansion of the combustion products and increase of pressure. Assuming that the geometry is such that the combustion products are trapped behind the frame front, a flow of unburned mixture is created. The flow interacts with obstacles generating a turbulent flow field. When the flame front propagates into the turbulent flow field the burning rate is increased significantly. This increased burning rate will further increase the flow velocity and turbulence at new obstructions a head of the flame. When a propagating flame front encounters repeated obstacles the positive feedback loop is circled several times. This mechanism of flame acceleration due to repeated obstacles may result in a very high overpressures (over 1 bar) within relatively short distances of flame propagation (less than 1 m).

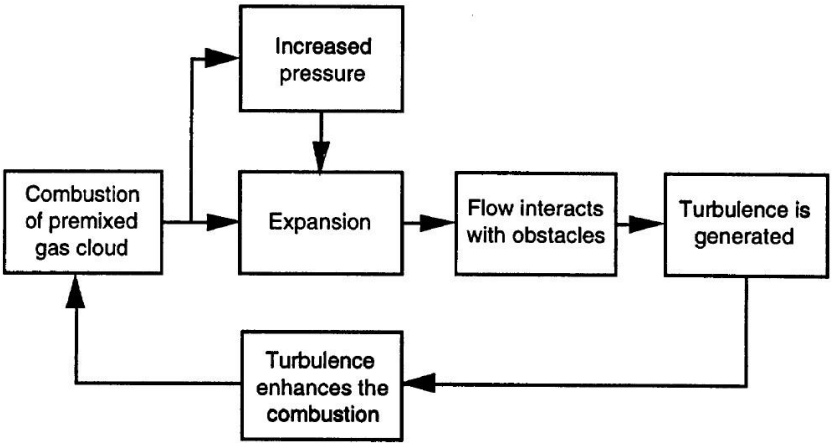

Fig. 9: Positive feedback loop causing acceleration due to turbulence [7].

II. Theoretical Model

2. Calculation of Detonation Parameters

2.1 Chapman - Jouguet (CJ) Model

Combustion wave moves at minimum speed consistent with conservation of mass, momentum and energy across the wave front with a relative velocity equal to the speed of sound (sonic or CJ condition). The detonation parameters are calculated by GASEQ software. Figure 10 shows computation results of Chapman-Jouguet parameters of propane and oxygen explosion.

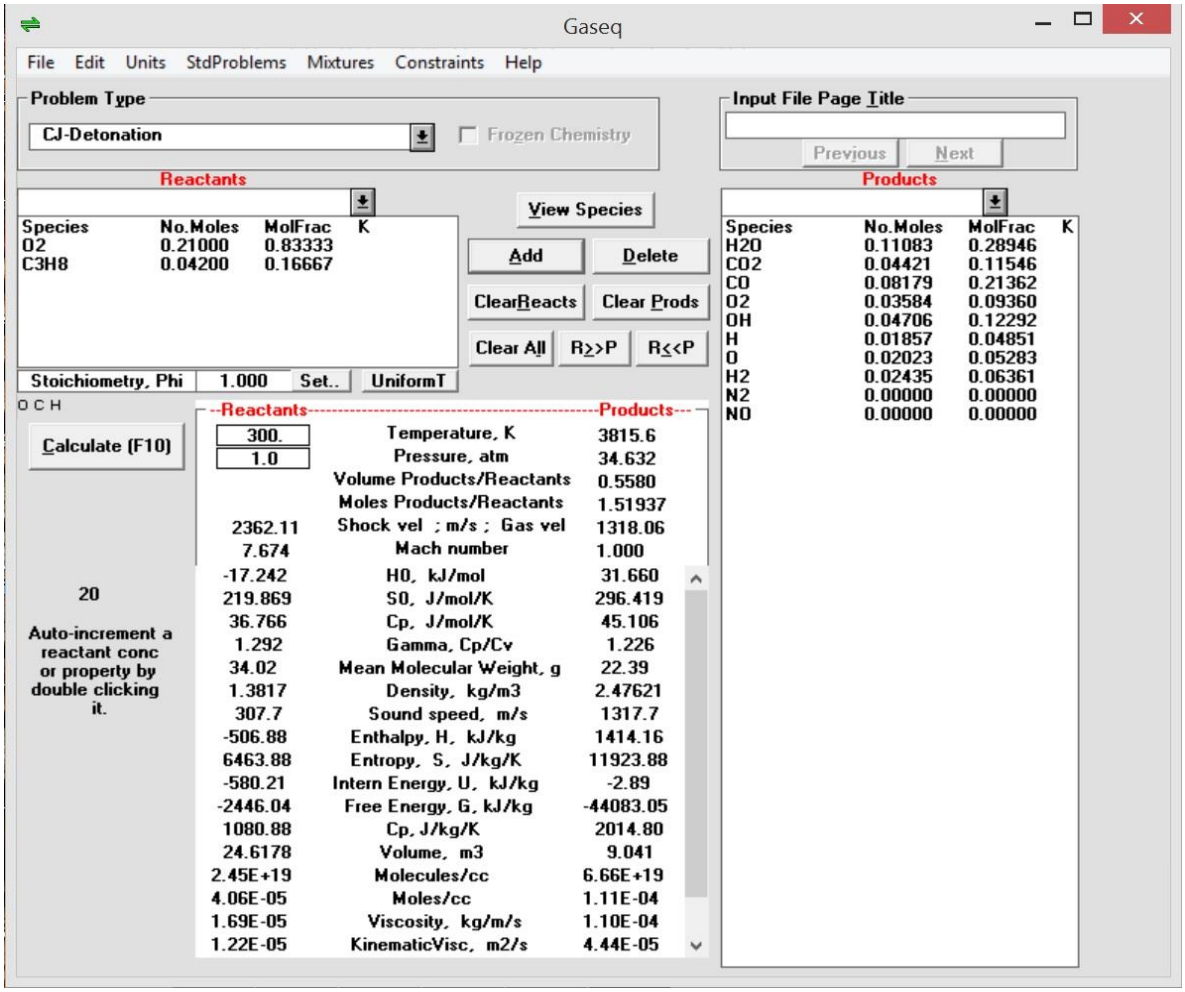

Figure 10: Calculation results of the parameters of Pentane and Oxygen.

Table 3 shows Chapman-Jouguet parameters of propane and oxygen explosion.

Table 3: Chapman-Jouguet parameters of gaseous mixtures [16]

Fuel		% (vol)	U_{CJ} (m/s)	P_{CJ} (bar)	S (mm)
Fuel-air mixtures					
hydrogen	H_2	29.6	1971	15.6	6–10
acetylene	C_2H_2	7.75	1867	19.1	10–15
ethylene	C_2H_4	6.54	1825	18.4	24–26
ethane	C_2H_6	5.66	1825	18.0	50–59
propane	C_3H_8	4.03	1801	18.3	40–60
methane	CH_4	9.48	1804	17.2	250–350
Fuel-oxygen mixtures					
hydrogen	H_2	66.7	2841	19.0	1–2
acetylene	C_2H_2	28.6	2425	34.0	0.1–0.2
ethylene	C_2H_4	25.0	2376	33.7	2-3
ethane	C_2H_6	22.2	2372	34.3	1–2
propane	C_3H_8	16.7	2360	36.5	0.5-1
methane	CH_4	33.3	2393	29.6	2-4

From figure 10 and table 3 we can see that the values of the detonation velocity and pressure of propane and oxygen mixture are similar. The detonation velocity which was obtained by GASEQ software is 2,362 m/s. The detonation velocity of the propane-oxygen mixture is 2,360 m/s. The detonation pressure which was obtained by GASEQ software is 34.6 atm. The detonation pressure of the propane-oxygen mixture is 36.6 bar (36.02 atm).

2.2 Estimation of the transport properties of the gaseous mixture

The mixture transport properties (density, thermal Diffusivity, kinematic viscosity, thermal conductivity & heat capacity) of the gaseous products can be calculated by STANJAN software (http://navier.engr.colostate.edu/~dandy/code/code-2/index.html).

3. Estimating the Effects of Gas Explosions

Explosions that occur in open air, known as "unconfined explosions" are fundamentally different—and require different countermeasures—than "confined explosions" which occur within some sort of containment. Confined explosions often occur in a process vessel or pipework, but may also occur in buildings. The explosion of a flammable mixture in a process vessel or pipework may be a detonation or a deflagration. The overpressure in a confined explosion is attributable to the expansion of the hot gases and may be exacerbated by the release of gases through an explosion vent (even a door or window) when the resulting turbulence produces a second pressure peak, as illustrated in Figure 11 [8].

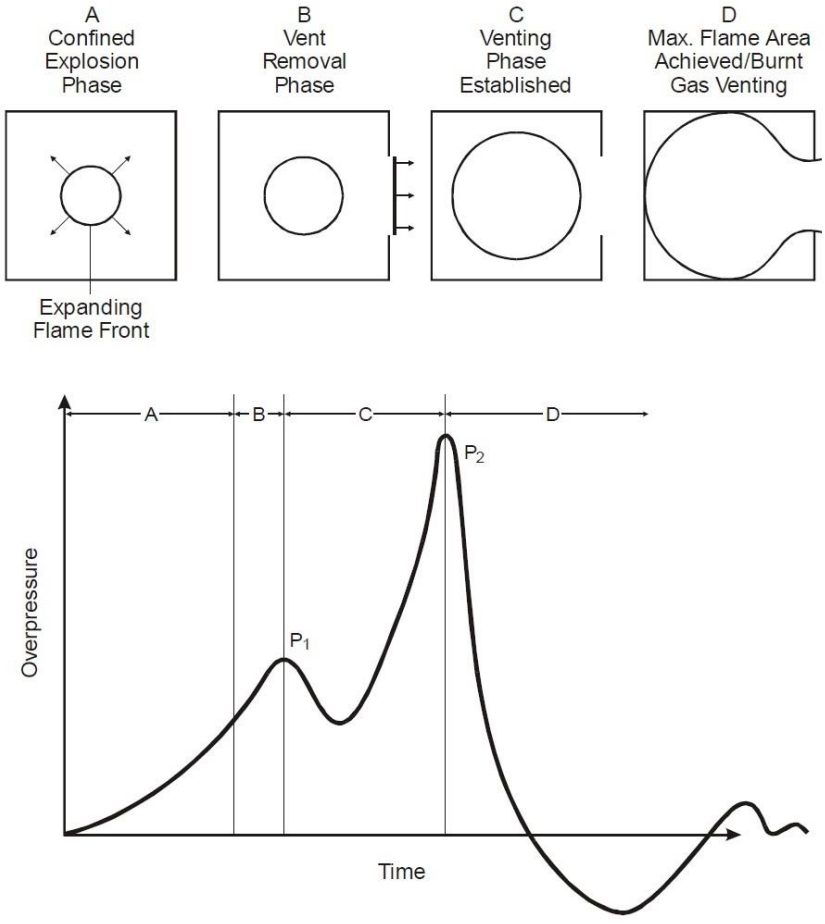

Fig. 11: Pressure peaks of gas explosion inside a building [8].

Confined explosion usually will not cause an accidental release of gas in any quantity directly into the atmosphere. Rather, such explosions usually release gases within some form of such as compartment or building of an industrial plant. If a flammable mixture forms and is ignited under these contained conditions, a confined gas explosion will occur. Moreover, if a gas is accidently released into the air, mixes with air and is ignited, the flame front travel through the mixture propagating in a spherical geometry whenever possible rather than remaining stationary, as illustrated in figure 12 [9].

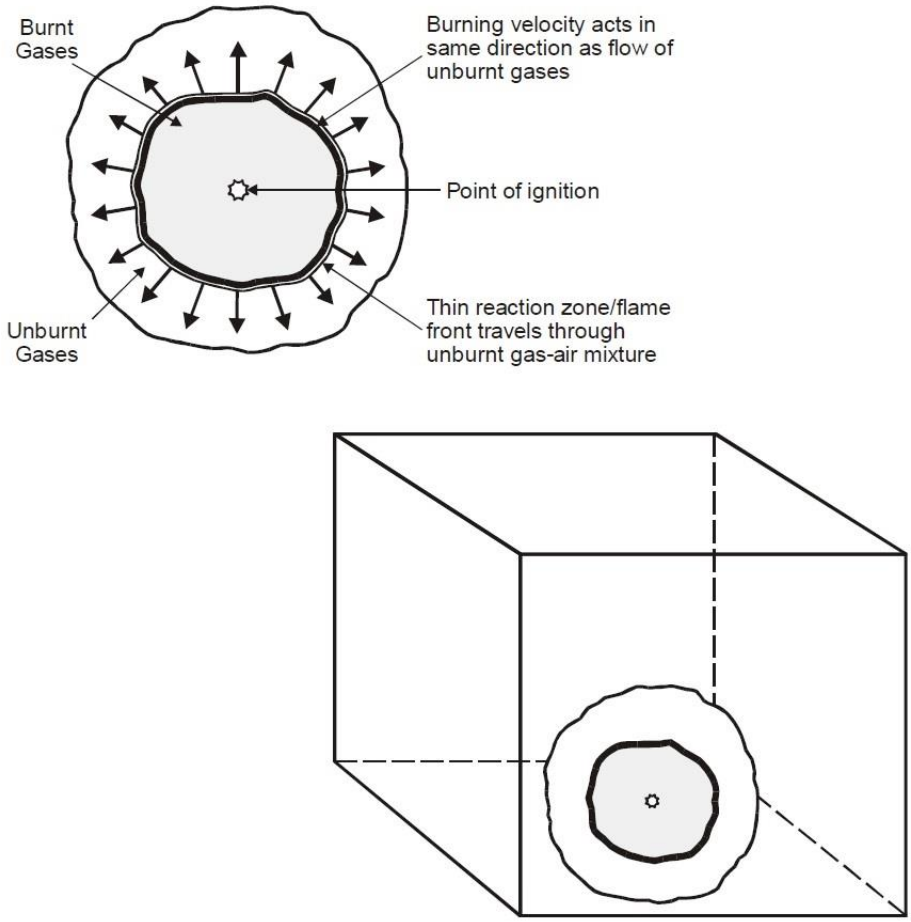

Fig. 12: Propagation of an explosion flame [9].

3.1 Estimating Explosive Energy Release in a Confined Explosion

One typical explosion in an enclosure is caused by flammable gas leaking, which mixes with air in the enclosure and subsequently ignites to cause an explosion. The energy released by expansion of compressed gas upon rupture of a pressurized enclosure may be estimated using the following equation [10]:

$$E = \alpha \Delta H_C m_F \qquad (8)$$

Where:

E – Explosive energy released in [kJ]

α – Yield

ΔH_c – Theoretical net heat of combustion [kJ/kg]

m_F – Mass of flammable vapor release [kg]

The yield, α, is typically in the range of 1-percent (0.01) for unconfined mass releases, to 100 percent (1.0) for confined vapor releases [10]. Table 4 presents the theoretical net heat of combustion for flammable gases [9].

Table 4: theoretical heat of combustion for several flammable gases [9].

Heat of Combustion, Ignition Temperature, and Adiabatic Flame Temperature* of Flammable Gases			
Flammable Gas	Heat of Combustion ΔH_c (kJ/kg)	Ignition Temperature T_{ig} °C (°F)	Adiabatic Flame Temperature T_{ad} °C (°F)
Acetylene	48,220	755 (1,391)	2,637(4,779)
Carbon monoxide (commercial)	10,100	765 (409)	2,387 (4,329)
Ethane	47,490	945 (1,733)	1,129 (2,064)
Ethylene	47,170	875 (1,607)	2,289 (4,152)
Hydrogen	130,800	670 (1,238)	2,252 (4,085)
Methane	50,030	1190 (2,174)	1,173 (2,143)
n-Butane	45,720	1025 (1,877)	1,339 (2,442)
n-Heptane	44,560	-	1,419 (2,586)
n-Octane	44,440	-	1,359 (2,478)
n-Pentane	44,980	-	1,291 (2,356)
Propane	46,360	1,010 (1,850)	1,281 (2,338)
Propylene	45,790	1,060 (1,940)	2,232 (4,050)
*Adiabatic flame temperature of lower limiting fuel/air mixture.			

3.2 TNT Mass Equivalent Calculations

One of the most common methods used to estimate the effects of an explosion is to relate the exploding fuel to trinitrotoluene (TNT). This method converts the energy contained in the flammable cloud into an equivalent mass of TNT, primarily because blast effects of TNT have been extensively studied as a function of TNT weight and distance from the source. Hence, we can infer the blast effects of an explosion by relating an explosion to an "equivalent" explosion of TNT. To do so, we relate a given fuel type and quantity to an equivalent TNT charge weight, as follows [10]:

$$W_{TNT} = \frac{W}{4500} \qquad (9)$$

Where:
W_{TNT} = weight of TNT (kg)
E = explosive energy released (kJ)

III. Proposed Algorithm To Estimate Blast Effects

The proposed algorithm is composed from the following steps:

1) Calculation of the gaseous concentration field and mass by using FDS software in order to estimate the minimal flammable gaseous concentration (see Table 1).
2) Calculation of the shock wave pressure loads on the walls
3) Estimation of structural integrity of the structure by using finite element software (FEA)

IV. Description Of Cfd Calculation Method

4.1 Calculation of the gaseous concentration field and mass by using FDS software

4.1.1 FDS Software

The fire dynamics simulator (FDS) has been developed at the Building and Fire Research Laboratory (BFRL) at the National Institutes of Standards and Technology (NIST), e.g. McGrattan et al. [11, 12]. The program calculates the temperature, density, pressure, velocity, and chemical composition within each numerical grid cell at each discrete time step. It computes the temperature, heat flux, and mass loss rate of the enclosed solid

surfaces. The latter is used in the case where the fire heat release rate is unknown. The following is a brief description of the major components of the model.

Hydrodynamic Model FDS code is formulated based on Computational Fluid Dynamics (CFD) of fire-driven fluid flow. The FDS numerical solution can be carried out using either a Direct Numerical Simulation (DNS) method or Large Eddy Simulation (LES). The latter is relatively low Reynolds numbers and is not severely limited in grid size and time step as the DNS method. In addition to the classical conservation equations considered in FDS, including mass species momentum and energy, thermodynamics based state equation of a perfect gas is adopted along with chemical combustion reaction for a library of different fuel sources.

Combustion Model For most applications, FDS uses a mixture fraction combustion model. The mixture fraction is a conserved scalar quantity that is defined as the fraction of gas at a given point in the flow field that originated as fuel. The model assumes that combustion is mixing controlled, and that the reaction of fuel and oxygen is infinitely fast. The mass fractions of all of the major reactants and products can be derived from the mixture fraction by means of "state relations," empirical expressions arrived at by a combination of simplified analysis and measurement [13].

Radiation Transport Radiative heat transfer is included in the model via the solution of the radiation transport equation for a non-scattering gray gas. In a limited number of cases, a wide band model can be used in place of the gray gas model. The radiation equation is solved using a technique similar to a finite volume method for convective transport, thus the name given to it is the Finite Volume Method (FVM) [13]. FDS also has a visual post-processing image simulation program named "smoke-view".

4.2 Calculation of the shock wave pressure loads on the wall

A detonation blast wave is usually referred to as an ideal blast wave or shock wave. It is led by a shock front when travelling through the air and compresses the fuel mixture or air in the front. The properties of the medium before and after the shock front can be related by the Rankine-Hugoniot relations. The shock wave characteristics can be defined by TNT explosion and scaling laws based on the charge weight and stand-off distance [14]. When blast waves encounter a rigid surface of an object they will reflect from it and, dependent on the size of the surface, diffract around it. The simplest case is that the blast wave impinges on an infinitely large rigid surface at zero angle of incidence β as shown in Figure 13 [14].

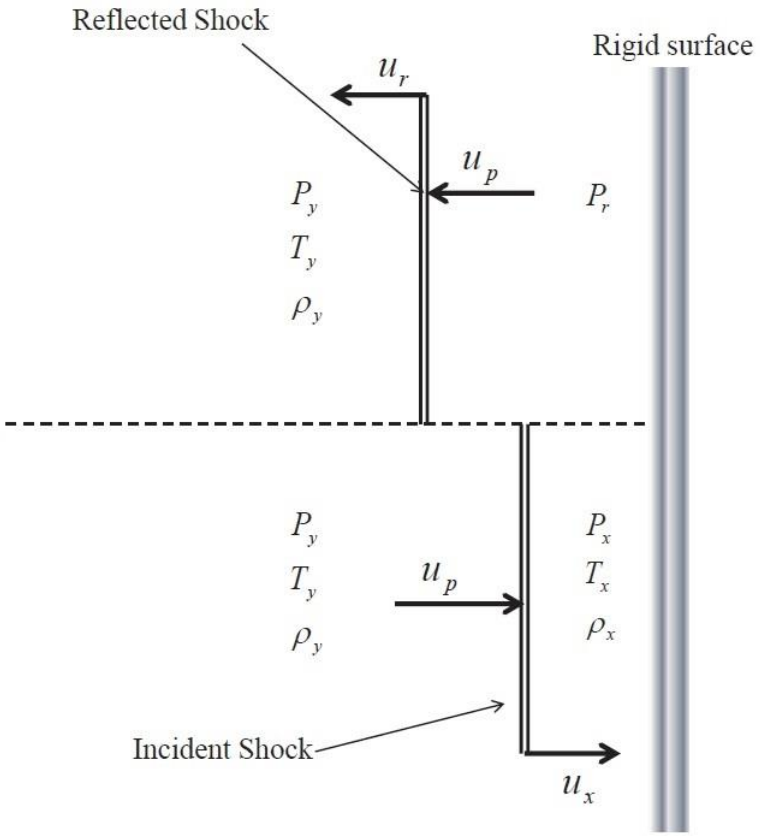

Fig.13: Normal reflected shock on a rigid surface [14].

In a normal reflection, the reflected pressure (p_r) can be defined in terms of the pressures across the incident shock front p_y and p_x as shown in Eq. (22) [14].

$$\frac{p_r}{p_x} = \frac{(p_r/p_x)\left[(3k-1)(p_y/p_x)-(k-1)\right]}{(k-1)(p_y/p_x)+(k+1)} = \frac{p_y(8p_y-p_x)}{p_x(p_y+6p_x)} \qquad (10)$$

k is the specific heat ratio (k=1.4 for air ideal gas). The magnitude of a reflection shock can be also expressed in term of reflection coefficient Λ and for a normal reflection, Λ_n, as defined in Eq. (23):

$$\Lambda_n = \frac{p_r}{p} = \frac{p_r - p_x}{p_y - p_x} = \frac{8p_y + 6p_x}{p_y + 6p_x} \qquad (11)$$

Figure 14 shows the reflection coefficient as a function of incident angle [15].

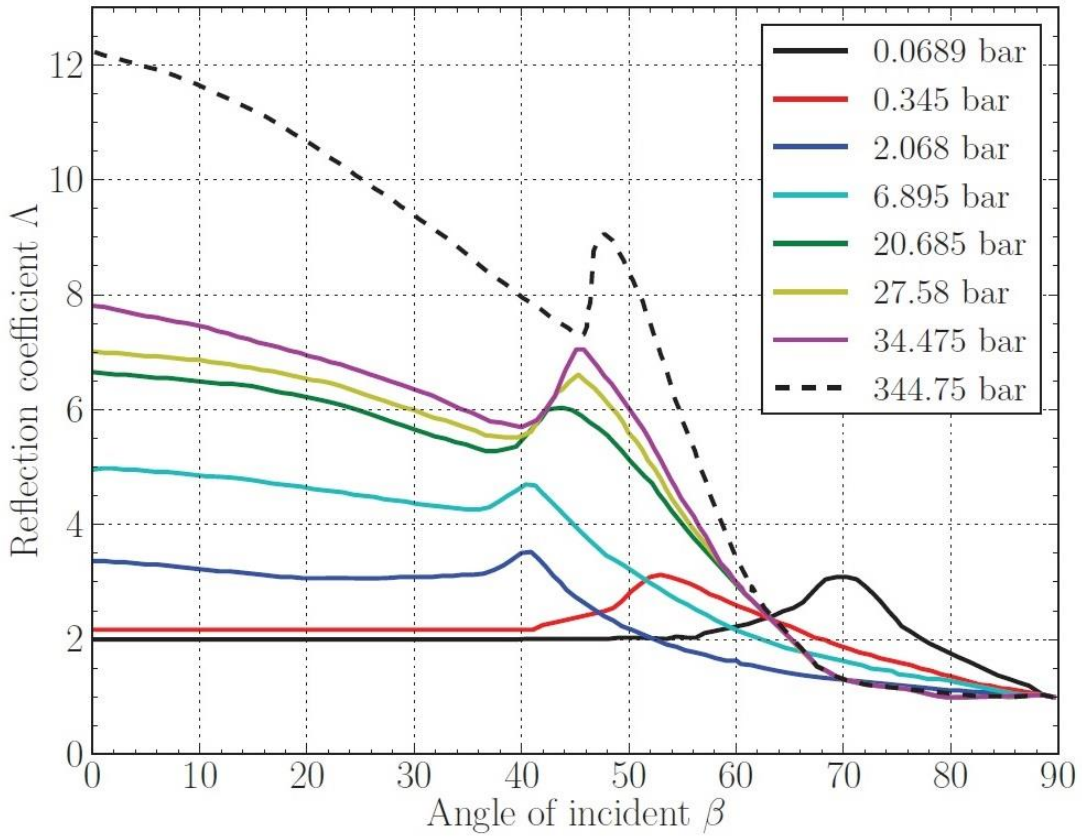

Fig. 14: Reflected pressure coefficients vs. angle of incidence (β) [15].

4.3 Consequences of forces

Loading becomes destructive when forces are sufficient to displace structures that are not anchored or else the forces (or thermal expansion) create stresses that exceed yield strength, σ_y, of the material. There are two kinds of loadings

(1) Mechanical loadings
(2) Thermal loadings

The thermal loadings cause thermal stresses inside the material. Thermal stresses are stresses that are created by differential thermal expansion caused by time-dependent heat transfer from hot explosion gases. This is distinct from the loss of strength of materials due to bulk heating, which is very important factor in fires which occur over very much longer durations than explosions [16].

$$\varepsilon = \sigma/E + \alpha\Delta T \qquad (12)$$

Figure 13 shows the typical Stress strain curve. The plot is in terms of engineering stress and strain, apparent maximum in stress is due area reduction caused by necking [16].

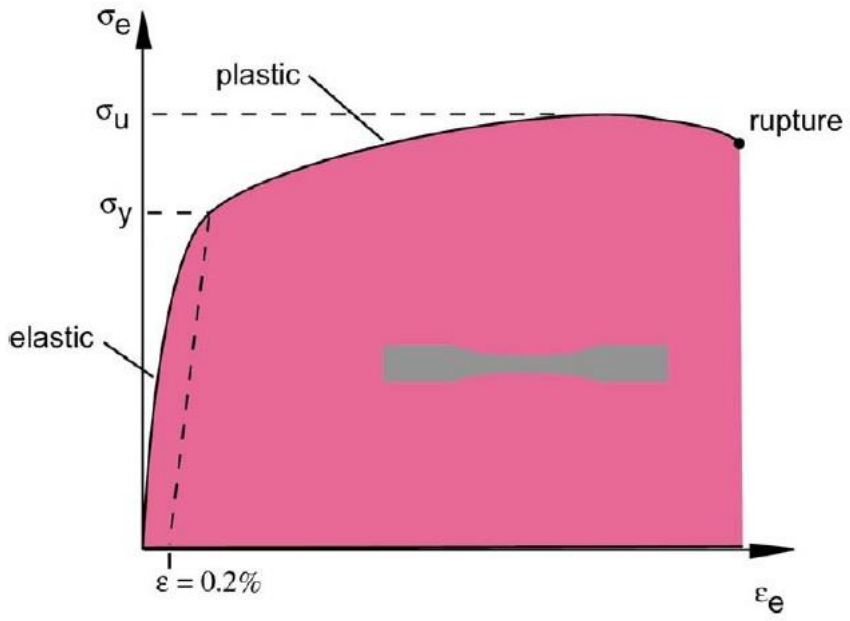

Fig. 15: Plot of stress as a function of relative strain [16].

Onset of yielding for: $\sigma \sim \sigma_y$

Necking occurs in plastic regime: $\sigma > \sigma_y$

Plastic instability and rupture for: $\sigma > \sigma_u$

Table 5 presents the mechanical properties of several materials [16].

Table 5: Typical material properties [16].

Material	ρ (kg/m3)	E (GPa)	G (GPa)	ν	σ_y (MPa)	σ_u (MPa)	$\varepsilon_{rupture}$
Aluminum 6061-T6	2.71 x 10^3	70	25.9	0.351	241	290	0.05
Aluminum 2024-T4	2.77 x 10^3	73	27.6	0.342	290	441	0.3
Steel (mild)	7.85 x 10^3	200	79	0.266	248	410-550	0.18-0.25
Steel stainless	7.6 x 10^3	190	73	0.31	286-500	760-1280	0.45-0.65
Steel (HSLA)	7.6 x 10^3	200		0.29	1500-1900	1500-2000	0.3-0.6
Concrete	7.6 x 10^3	30-50			20-30	-	0
Fiberglass	1.5-1.9 x 10^3	35-45			-	100-300	-
Polycarbonate	1.2-1.3 x 10^3	2.6			55	60	-
PVC	1.3-1.6 x 10^3	0.2-0.6			45-48	-	-
Wood	0.4-0.8 x 10^3	1-10			-	33-55	-
Polyethylene (HD)	0.94-0.97 x 10^3	0.7			20-30	37	-

4.4 Estimation of structural integrity of the structure

Many guidelines and codes have been published for design of structure to resist accidental blast loading. Most of the codes are based on Biggs' single degree of freedom model and covering both determination of blast loading and structural response. Structure to resist the effects of accident explosions is presented in UFC 3-340-02 [15]. This code is the most widely used publication in both military and civilian organizations for design of structures to prevent blast damage to structure or personnel from accidental explosions. It establishes design procedures and construction techniques whereby propagation of explosion or destructive detonation can be mitigated. It includes information on blast, shock loading prediction, principles of dynamic analysis and reinforced concrete/steel design for blast.

V. Conclusion

Unexpected releases of combustible vapors/gases can lead to explosions, which threaten the integrity of equipment and structures. Multiple explosions can destroy plants, jeopardize lives, and inflict large economic losses; outdated parts of the pipe system can leak flammable gas in air and pose the danger of explosion. Therefore, it is important to be able to predict explosion properties and to design pipes and storage tanks that can withstand such catastrophic events. Such efforts enable plant engineers to evaluate risks associated with their designs subject to various possible explosions. Pressure rises almost instantaneously because of the overpressure from an explosion causing structural damage or deformation of pipes and storage tanks. Explosive pressure and structural damage can be estimated with analytical and numerical tools. By using these computational tools, safe distances between equipment and structures can be assigned. In this work an algorithm has been developed in order to estimate the structural damage. The proposed algorithm is composed from the following steps:

1) Calculation of the gaseous concentration field and mass by using FDS software
2) Calculation of the shock wave pressure loads on the walls
3) Estimation of structural integrity of the structure

References

[1]. Bang, B., Park, H., Kim, J., Al Deyab S.S., Yarin, A.L., Yoon, S.S., Analytical and numerical assessments of local overpressure from hydrogen gas explosions in petrochemical plants, Fire and Materials: 2016, DOI: 10.1002/fam.2390.

[2]. Coco J. The 100 Largest Losses (1972–2001): Large Property Damage Losses in the Hydrocarbon-Chemical Industries. 20th Edition: Marsh Property Risk Consulting 20th Edition. A Publication of Marsh's Risk Consulting Practice: New York 2003.

[3]. Kletz T., What Went Wrong? Case Histories of Process Plant Disasters and How They Could Have Been Avoided. Butterworth-Heinemann: Oxford, 2009.

[4]. Mallard E. and Le Chatelier H. L., Sur la vitesse de propagation de l'inflammation dans les melanges explosifs, *Compt. Rend. Acad. Sci. Paris*, 93, 145–148 (1881).

[5]. Berthélot M. and Vieille P., Sur la vitesse de propagation des phenomenes explosifs dans le gaz, *Compt. Rend. Acad. Sci. Paris*, 93, 18 (1881).

[6]. Lewis, B. & Von Elbe, G., Combustion Flames and Explosion of Gases, Second Edition, *Academic Press Inc.*, New York and London, 1961.

[7]. Luatkaski, R., Understanding vented gas explosion, *VTT Energy, Technical Research Center of Finland Espoo*, 1997.

[8]. Harris, R.J., The Investigation and Control of Gas Explosions in Building and Heating Plant, British Gas, 1983.

[9]. Iqbal, N. & Salley, M.H., Fire Dynamics Tools (FDT^s) Quantitative Fire Hazard Analysis Methods for the U.S. Nuclear Regulatory Commission Fire Protection Inspection Program, NUREG-1805, Vol. 1, *Prepared for Division of Systems Safety and Analysis Office of Nuclear Reactor Regulation U.S. Nuclear Regulatory Commission Washington, DC 20555-0001*, June 2003.

[10]. Zalosh, R.G., Explosion Protection," Section 3, Chapter 16, *SFPE Handbook of Fire Protection Engineering*, 2nd Edition, P.J. DiNenno, Editor-in-Chief, National Fire Protection Association, Quincy, Massachusetts, 1995.

[11]. McGRATTAN, K. Fire Dynamics Simulator (Version 5) - Technical Reference Guide Volume 1: Mathematical Model, NIST Special Publication 1018, NIST, (2010).

[12]. McGRATTAN, K., FORNEY, G.P., Fire Dynamics Simulator (Version 5) - User's Guide. NIST Special Publication 1019, NIST, (2010).

[13]. McGRATTAN, K., 2005, Numerical Simulation of the Caldecott Tunnel Fire, April 1982, NISTIR 7231.

[14]. Chen, A., Structural Response to Vapor Cloud Explosions, A thesis submitted for the degree of *Doctor of Philosophy*, Department of Civil and Environmental Engineering Imperial College London, 2014.

[15]. Structures to Resist the Effects of Accidental Explosions, UFC 3-340-02, 5 December 2008.

[16]. Shepherd, J.E. Structural response to explosions, *Presented at 1st European Summer School on Hydrogen Safety University of Ulster*, August 2007.

Alon Davidy "Modelling Confined Hydrocarbon Gas Explosions Part I: Algorithm Development." IOSR Journal of Mechanical and Civil Engineering (IOSR-JMCE) , vol. 15, no. 1, 2018, pp. 48-63